XPS Characterization and Morphology of MgO Thin Films grown on Single-Crystalline Diamond (100)

S. M. Lee[*], T. Ito[**] and H. Murakami[**]

Technology Research Institute of Osaka Prefecture Ayumino 2-7-1, Izumi, Osaka 594-1157, Japan[*]

Osaka Univ.[**]

Abstract

Morphology and composition of MgO films grown on single-crystalline diamond (100) have been studied. MgO thin films were deposited in the substrate temperature range from room temperature (RT) to 723K by means of electron beam evaporation using MgO powder source. Atomic force microscopy images indicated that the film grown at RT without O_2 supply was relatively uniform and flat whereas that deposited in oxygen ambient yielded higher growth rates and rough surface morphologies. X-ray photoelectron spectroscopy analyses demonstrate that the MgO film deposited at RT without O_2 has the closest composition to the stoichiometric MgO, and that a thin contaminant layer composed mainly of magnesium peroxide (before etching) or hydroxide (after etching) was unintentionally formed on the film surface, respectively. These results will be discussed in relation to the interaction among the evaporated species and intentionally supplied oxygen molecules at the growth front as well as the interfacial energy between diamond and MgO.

Key words : MgO, Diamond, XPS, Magnesium peroxide, Magnesium hydroxide

1. Introduction

The properties of ultra-thin metal oxide films have received considerable attention because of their important applications in the heterogeneous chemical catalysis or microelectronics field[1,2]. For example, highly oriented MgO thin films have been widely used as structural templates for textured growth of other oxide films such as ferroelectrics[3] and high temperature super-conductors[4]. Furthermore, it was recently reported that the insertion of a ultra-thin insulating layer such as MgO or LiF between a low-work-function electrode and an electron transport layer in light emitting diode structures led to a decrease of the onset voltage as well as an increase of the light emission efficiency[5]. However, it is well known that such insertion of a different material or hetero-structure growth often leads to significant problems such as alloying, defect creation and nonuniform growth near the interfaces.

MgO crystal is composed of closed-shell ions with a rocksalt structure. It has been usually recognized that MgO is chemically stable since an experimentally measured band gap is about 7.8eV[6]. However, it turned out that the MgO surface is rather reactive with other atoms, which obviously differs from LiF or NaCl with a chemically stable surface. This may be related to the divalent nature of its constituents and the ability to form a single (Mg-O) or double bonds (Mg=O) between Mg and O atoms. The Mg-O type bonding involves two unpaired electrons[7], so that the constituents are not in the fully closed-shell but able to form stable bonds with other species. In earlier articles, it has been reported that magnesium peroxide (MgO_2)[8,9] or hydroxide ($Mg(OH)_2$) [10] are usually formed on MgO film surfaces. We will also discuss these possibilities in this work.

We have deposited MgO thin films on homoepitaxial diamond under various conditions and investigated the compositions and morphologies using X-ray photoelectron spectroscopy (XPS) and an atomic force microscope (AFM).

2. Experimental

High-pressure and high-temperature synthesized (HPHT) single-crystalline (100) diamond was used as substrates. Undoped and B-doped single-crystalline diamond films with respective thickness of ~ 0.6 μm were subsequently grown by a conventional microwave-plasma chemical-vapor-deposition (MPCVD) method. Then, onto the diamond substrates thus grown, MgO thin films were deposited at substrate temperatures ranging from room temperature (RT) to a high temperature (HT) of 723 K using an electron beam evaporator[11] with a target material of MgO powder with a purity of 99.99%. This process was expected to give reasonably good uniformity over the whole substrate surface of 3×3 mm^2. The base pressure of deposition chamber was ~5×10^{-7} Torr and oxygen gas of ~3×10^{-5} Torr was introduced into the deposition chamber in case of oxygen ambient depositions.

XPS spectra were acquired using a high-spatial resolution apparatus with Mg-Kα X-rays (model: Kratos AXIS-165). The diameter of sampling areas measured was about 100 μm. The pass energy of the spectrometer was set to 40 eV, giving a system energy resolution of ~ 0.89 eV and an energy reproducibility of 25 meV. A work function of the XPS spectrometer was estimated so as for the binding energy of Au f$_{7/2}$ peak to be 84.0 eV[12]. Since the Fermi levels of the sample and the spectrometer were not always in equipotential due to possibly charging up, the binding energy of Mg2p level was assumed to be 50.3 eV in case of single-crystalline MgO (100) surfaces[9] while the C1s level of unintentionally absorbed C species was used to calibrate binding

energies in case of deposited MgO films. Since the XPS chamber was separated from the film deposition chamber, surface contamination of the film possibly occurred during the sample handling in air. For removal of this contaminant-covered layer, Ar ion bombardment was carried out just before the XPS measurements. Ion gun was used at an acceleration energy of 4.0 kV and ionic current of = 1μA in Ar gas ambient of 1 ~ 2$\times$ 10^{-7} Torr to lightly sputter the specimen surfaces.

3. Results and Discussion

3.1 Surface morphology of deposited MgO films

3.1.1 Without oxygen supply

Figure 1(a) shows a typical AFM image of the MgO film deposited at RT without oxygen supply. The nominal deposition thickness was estimated as 3 nm. The surface was relatively uniform and flat over the whole area measured. The RMS was 2.5 nm, meaning that the MgO film grown became flatter than the original surface of the B-doped diamond substrate (RMS : 3.4 nm).

Figure 1(b) shows a typical AFM image of the film deposited at 723 K without oxygen supply. Although the nominal deposition film thickness was about 20 nm, the RMS measured was ~25 nm, indicating that the HT deposition resulted in enlarged surface roughness, compared with the RT deposition without oxygen supply. The films deposited at HT without oxygen supply represented a lower growth rate than that of the oxygen-ambient HT deposition. The formation of these MgO islands is considered to result from high-speed migration of deposited species in the case of the HT growth and a relatively large interfacial free energy between diamond and MgO.

3.1.2 With oxygen supply

MgO films deposited in oxygen ambient represented substantially rough surfaces even for the RT deposition specimens, as shown in Fig.

1(c). The RMS of a ~5-nm thick film markedly increased up to 66 nm and the lateral size of the round-shape domains was also enlarged, compared with the other MgO films examined, meaning that the MgO islands preferably grew in the oxygen ambient.
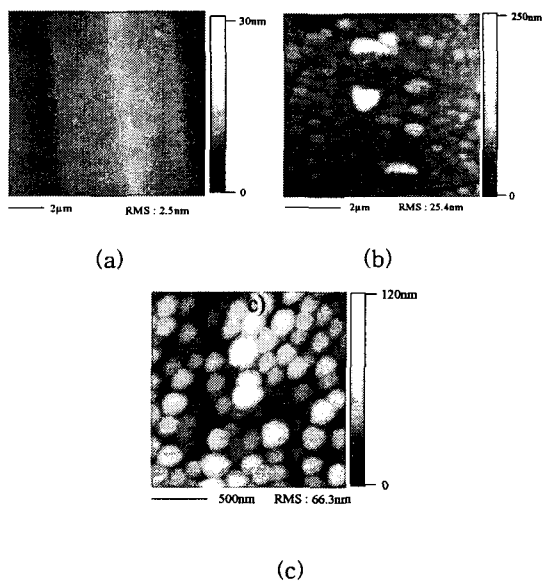

(a)   (b)

(c)

Fig. 1. Typical AFM images of MgO films (a) deposited at room temp. (RT) and (b) high temp. (HT) of 723 K without oxygen. (c) is the film surface deposited at RT in oxygen ambient.

3.2 XPS analysis of single-crystalline (100) MgO

In order to obtain reference data for the stoichiometric MgO in bulk, Mg2p and O1s XPS spectra were taken for both as-received and sputter-cleaned surfaces of single-crystalline (100) MgO. Ion etching was carried out for two minutes in every etching sequence. Typical results are shown in Figs. 2 (a) and (b). The Mg2p spectrum appeared as one peak at the binding energy of 50.3 eV, which was hardly influenced by the ion etching performed. On the other hand, the O1s
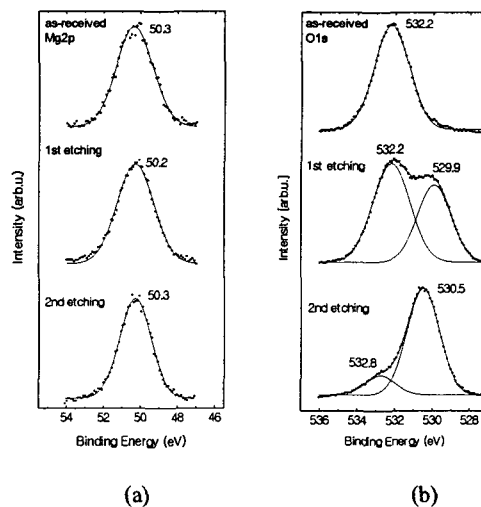

(a)   (b)

Fig. 2. XPS spectra of (a) Mg2p and (b) O1s photoelectrons taken from single-crystalline (100) MgO. Spectra from the top to bottom correspond to those of as-received (before sputtering) surface, after 2-min and 4-min sputtering, respectively. Curves (thin dotted lines) demonstrate gaussian components deconvoluted and their sum (thick dotted lines).

spectrum was composed of two peaks which were located at 530.5 eV and 532.8 eV for the lower binding energy (LBE) peak and the higher (HBE) one, respectively. The surfaces of as-received specimens had only one HBE peak. As the ion etching was progressed, the LBE intensity increased while the HBE one decreased. For a surface twice etched, the intensity of the LBE peak was significantly larger than that of the HBE peak. Similar relative intensities between the LBE and HBE components were observed for the surfaces etched more than two times. Therefore, it is concluded that the LBE peak came from the single-crystalline MgO bulk phase with negligible sputtering damages while the HBE one for as-received specimen originated from the

contaminant layer unintentionally formed on the MgO surface. The observed energies of HBE and LBE components are in good agreement with XPS data previously published for MgO films. For example, the Mg2p peak was located at 49.5 – 49.7 eV for metallic Mg while ~ 50.8 eV for MgO[9]. On the other hand, Jupile et al. investigated O1s core levels of alkaline metal oxides by comparing binding energy differences between the valence band and the core level[13]. The O1s binding energies reported were typically located at 527 ~ 531 eV and 530 ~ 532 eV for alkaline metal oxide (O^{2-}) and peroxide (O_2^{2-}), respectively. However, binding energy differences between those components were almost unchanged[10,13]. This identical difference in binding energy or chemical shift is originated from an appreciable change of the electronic charges surrounding O atoms between the O^{2-} and O_2^{2-} configurations.

3.3 XPS analysis of deposited MgO thin films

3.3.1 O 1s spectra

Figures 3 (a) and (b) show typical O1s spectra of the MgO films deposited under various conditions. The LBE peaks were located at binding energies of 529~531 eV, which were assigned to O^{2-} in MgO by applying the above results of single-crystalline MgO. On the other hand, the HBE peaks were located at 532~533 eV, being higher about 2~2.5 eV than the corresponding LBE one, and the HBE intensities significantly decreased after the ion etching in all the cases examined. Here, it should be noted that since the MgO crystal surface is not in the full closed-shell electronic structure, it remains chemically reactive. As a matter of fact, it is theoretically verified that the ground states of MgO are not composed of the highly ionic configuration described mainly as double-bonded Mg=O (or Mg^{2+} and O^{2-}) but are rather well described as single-bonded Mg-O with two unpaired electrons[7]. Therefore, there possibly

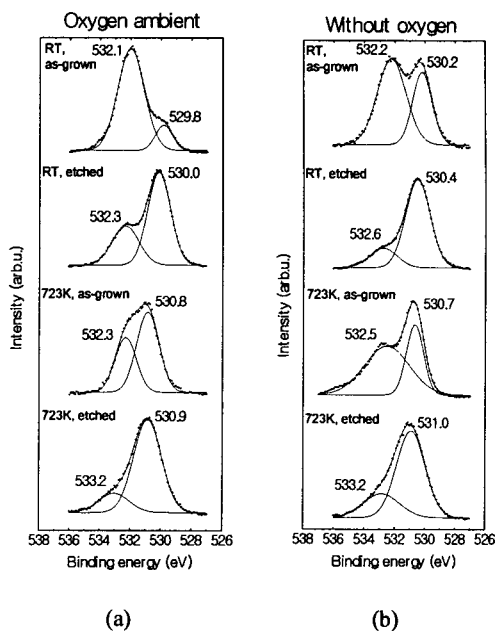exist different energy states from the bulk ones on the MgO film surface. As discussed in earlier

Fig. 3. O1s XPS spectra of MgO thin films deposited (a) without and (b) with intentional oxygen supply. The upper two spectra were taken from a room temperature (RT) deposited specimen while the lower two from a 723-K deposited specimen. All the specimens were investigated before (as-grown) and after 4-min ion etching with 4-keV Ar ions (etched). Curves (thin dotted lines) show gaussian components deconvoluted and their sum (thick dotted lines).

studies, the following two cases are considered as such surface layers giving the HBE peak. The first one corresponds to the case where since the film surface was exposed to oxygen after the film deposition in the chamber and during the sample handling in air for the subsequent XPS measurements, a peroxide layer was mainly formed on the MgO film surface. Huang et al.[14] found that an increase of oxygen supply in the Mg oxidation process resulted in an appreciable

increase of the HBE peak intensity of O1s spectrum. Wang et al.[15] confirmed that a peroxide layer was formed on single-crystalline MgO surfaces. In the present case (see Fig. 3), for both the as-grown and ion-etched RT-deposited specimens, the HBE components had higher intensities for the oxygen-ambient-deposited films than for ones without oxygen supply. Especially, the HBE component of the as-grown film deposited at RT in oxygen ambient had a remarkably high intensity. This should be closely related to the surface morphology and the surface reactivity. Generally, it is recognized that the kinetics of oxygen adsorption or chemisorptions is strongly influenced by both surface roughness and film quality[16]. Thus, since the RT-deposited film in oxygen ambient represented the highest roughness, as shown in Fig. 1, a relatively thick peroxide layer was easily formed just after the film deposition by the supplied oxygen or during the sample transferring. Also, the substrate film property have an important effect on the contaminant layer formation. which could be recognized from that the surface contaminant amount of HT-deposited film was smaller than RT one, although the roughness is higher than RT ones. (see Fig. 3)

The other case is like as follows. Because the main residual gas component is hydrogen in the XPS chamber, a hydroxide layer is easily formed on the sputtered MgO surfaces and also give the O1s HBE peak. Since the ion bombardment probably create a considerable number of dangling bonds in the MgO surface region, the surface become more reactive with other atoms. We observed time variations of the O1s spectra after the ion etching, as shown in Fig 4. The specimens were kept after 4-min ion sputtering for one hour in the XPS chamber with a vacuum pressure of ~ 4×10^{-10} Torr. The intensity ratios of HBE to LBE, I_{HBE}/I_{LBE}, once remarkably decreased just after the etching and slightly increased as the vacuum keeping time passed.

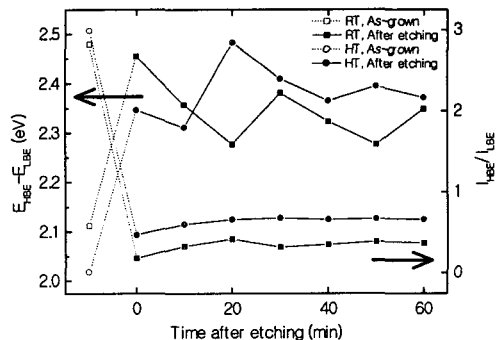After about 20-min storages, the intensity ratios became constant. The HT-deposited film

Fig. 4. Intensity ratios and binding energy differences of HBE and LBE components of O1s XPS peaks measured, I_{HBE}/I_{LBE}, as a function of the storage time after the Ar ion etching. The MgO films were deposited at room temperature (RT) and a high temperature of 723K (HT) without oxygen. 4-keV Ar ion etching was carried out for 4 min in each case.

represented a larger (saturated) intensity ratio of I_{HBE}/I_{LBE} than the RT-deposited one. These indicate that the hydroxide film was more easily formed on the HT-deposited MgO films than on the RT-deposited ones whereas the thickness of the newly formed layer was limited. A possible reason for this is related to surface roughness and slightly O-rich compounds of the HT-deposited film as described below.

Then, the thickness of such sputter-induced layer was roughly estimated using the ratio I_{HBE}/I_{LBE} of the O1s photoelectrons by assuming uniform thickness and negligible elastic scattering. Using O1s signals of I_{OH}^{O} and I_{O}^{O} coming from the hydroxide overlayer (OH) on the MgO substrate (O), respectively, the overlayer thickness d_{OH} is approximately given by

$$d_{OH} = \lambda^O \cos\theta \ln\left(\frac{I_{OH}^O I_O^{O\infty}}{I_O^O I_{OH}^{O\infty}} + 1 \right) \quad (1)$$

where λ^O is the escape depth of O1s photoelectrons in the over layers and substrate, θ the photoelectron emergency angle from the surface normal, and $I_i^{O\infty}$ the O1s signal (areal) intensities of the corresponding pure materials i [17]. Here, O and OH means oxide and hydroxide, respectively. The escape depth for O1s electrons excited by Mg-Kα X-rays λ^O was assumed to be 1.09 nm in both the surface oxide layer and the bulk MgO[18] and θ was approximately 0° in the present XPS apparatus used. Since the sensitivity factor of O1s photoelectrons are essentially the same for pure hydroxide ($I_{OH}^{O\infty}$) and mono oxide ($I_O^{O\infty}$), the intensity ratio become 0.75. The intensity ratios of I_{OH}^O / I_O^O (or I_{HBE}/I_{LBE}) actually measured for the RT-deposited film fell in the range of 0.35 ～ 0.45, as shown in Fig. 4. The overlayer thickness of RT-deposited film calculated from Eq. (1) was about 0.15 nm immediately after the ion etching and increased to 0.25 ～ 0.32 nm for a further storage in the XPS chamber. Since the Mg-O bond length in hydroxide (Mg(OH)$_2$) is about 0.24 nm, the thickness of the sputter-induced hydroxide layers was estimated to be < 1.5 ML.

On the other hand, it is considered that although the binding energy difference of O1s spectrum between hydroxide and peroxide is rather small, a suitable procedure makes it possible to deconvolute each spectrum. In order to compare the binding energies observed for the as-grown and ion-sputtered surfaces in more details, the energy difference between the HBE and LBE peaks, $E_{HBE} - E_{LBE}$, are also plotted in Fig. 4 as a function of the storage time in the UHV chamber. After the ion etching, the energy differences ranged from 2.27 to 2.48 eV, being

about 0.2～0.3-eV larger, compared with those of the as-grown films without sputtering. This strongly suggests that the surface layer newly formed after the sputtering is mainly composed of hydroxide. since O atoms in peroxide are mainly bonded with ionic bonding while O-H bonds in hydroxide are substantially covalent bonding, the HBE peak for hydroxide has a slightly larger binding energy (or a less chemical shift from the stoichiometric MgO (mono oxide) state) than that for peroxide. These energy differences were well reproduced although the values were so small.

3.3.2 Mg 2p spectra
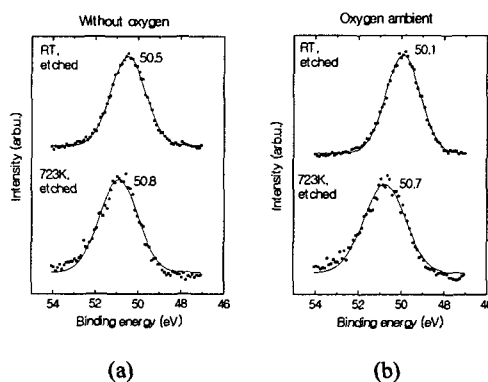

(a)   (b)

Fig. 5. Mg 2p XPS spectra of MgO films deposited (a) without and (b) with intentional oxygen supply. The upper ones were taken from a specimen grown at room temperature (RT) while the lower ones from specimens grown at 723 K. The terms of "as-grown" and "etched" mean before and after 4-min ion etching with 4-keV Ar ions, respectively.

Figures 5 (a) and (b) show Mg2p spectra taken from the MgO films deposited under the various conditions. The binding energies after a light sputtering were located in the range of 50.1～50.8 eV, being in good agreement with that of the single-crystalline MgO. The Mg2p spectra were

represented only by a single peak for all the specimens differently grown. This indicates that since Mg atoms in oxide, peroxide and hydroxide have almost the same charge distribution as Mg^{2+}, the Mg2p XPS spectra observed cannot be well deconvoluted to these three components. On the other hand, it is found that the Mg2p binding energy of the HT-deposited film shifted by ~0.9 eV to the higher binding energy side than that of the RT-deposited film.

This may be interpreted in terms of Fermi level shift and band bending[19]. In the case of the ideal MgO crystal, Fermi level may be located around in the middle of the band gap. Deficiency of O or a slight enrichment of Mg in the MgO film grown may tend to the Fermi level of the specimen to move up towards the conduction band minimum. As described in section (c), it is found that slightly Mg-rich compositions were presented for the RT-deposited specimens while the HT-deposited specimens were slightly O-rich. Furthermore, some other variations such as the initial/final state effects, possible interface properties and chemical modifications[9] can additionally alter the chemical potential and electronic structure. Thus, a more detailed interpretation of the core level shifts may not be so meaningful because of the significant amount of sputter-created defects in the surface layer.

3.3.3 Chemical composition of deposited MgO films

The stoichiometry of the deposited MgO thin films underlying below the contaminated layer can be estimated by comparing the areal intensity ratios of Mg2p peak to O1s peak, I^{Mg}/I^O, on the basis of the corresponding I^{Mg}_{cry}/I^O_{cry} from the sputtered single-crystalline (100) MgO, the bulk of which is reasonably assumed to have one-to-one stoichiometry. The differences in photo-ionization cross-sections, energy-dependent analyzer transmission factors and escape depths

and so on should be considered for the spectral intensity calculations. Here, λ^O of 1.09 nm was employed while the escape depth for Mg2p ones λ^{Mg} was derived from the kinetic energy (E_{kin}) dependence of photoelectrons as $(E_{kin})^{1/2}$. Since the film surface roughness has a substantial effect on the XPS spectral intensities, we firstly estimated a morphology factor as follows. After a sufficient ion etching, a thin $Mg(OH)_2$ layer with the same thickness as in the case of the single-crystalline MgO is assumed to be formed uniformly in a fraction s of the analyzed area of the MgO film, while the remaining analyzed area with the fraction of 1-s is assumed to be sufficiently thick $Mg(OH)_2$ region due to the surface undulations or the island shape domains (case 1). As the surface become flatter, s will be closer to unity as in the case of the single-crystalline MgO. Under these assumptions, the O1s intensity ratios of $Mg(OH)_2$ to MgO, I^{OH}_O/I^O_O, in the analyzed volume can be written using conventional exponential decays of photoelectron intensities as

$$\frac{I^O_{OH}}{I^O_O} = \frac{1.34}{s}\left(e^{-\frac{d_{OH}}{\lambda^O \cos\theta}} - s \right) \qquad (2)$$

where d_{OH} is the thickness of the $Mg(OH)_2$ layer formed on the MgO film[20]. Here, I^O_{OH} is composed of $s \cdot I^O_{OH}$ from the thin $Mg(OH)_2$ region and $(1-s) \cdot I^O_{OH}$ from the thick $Mg(OH)_2$ region, while I^O_O is $s \cdot I^O_O$ from the underlying thick MgO film. The s values obtained from Eq. (2) are listed in Table I. The RT (without O_2)-deposited film has the closest composition to the single-crystalline MgO, which is well consistent with the surface morphology results (RMS). Then, using these s values as

morphology factors, spectral intensity ratios of the deposited MgO films, I^{Mg}/I^O, have been calculated. These will be represent the deviation from the stoichiometry of MgO film well.

$$\frac{I^{Mg}}{I^O} = \qquad\qquad\qquad (3)$$

$$\frac{\alpha\lambda^{Mg}}{\lambda^O}\;\frac{D_{OH}^{Mg} + s\left(D_{OX}^{Mg} - D_{OH}^{Mg}\right)\exp\left(\dfrac{-d}{\lambda^{Mg}\cos\theta}\right)}{D_{OH}^{O} + s\left(D_{OX}^{O} - D_{OH}^{O}\right)\exp\left(\dfrac{-d}{\lambda^{O}\cos\theta}\right)}$$

where α corresponds to the relative sensitivity factor determined by energy-dependent analyzer transmission factor and the relative photo-ionization cross-section between Mg2p and O1s photoelectrons, D_{OH}^{Mg} and D_{OX}^{Mg} are the Mg densities, D_{OH}^{O} and D_{OX}^{O} are the O densities in the Mg(OH)$_2$ layer and the underlying MgO$_x$ film, respectively. If the stoichiometric MgO and Mg(OH)$_2$ are considered, D_{OH}^{Mg} and D_{OH}^{O} are approximately 0.67 D_0^{Mg} and approximately 1.34 D_0^{O} respectively. Here, D_0^{Mg} and D_0^{O} are the Mg and O densities of the stoichiometric MgO, respectively. From the measured intensity ratio of I^{Mg}/I^O, the atomic composition of the deposited MgO$_x$ film was roughly estimated using Eq. (3). The results are listed in table I. Oxygen rich compositions appeared in the case of the HT-deposited specimens. On the other hand, the RT-deposited films were almost stoichiometric or slightly Mg-rich. It should be noted that the RT (without O$_2$)-deposited film had the composition closest to the single-crystalline MgO. Furthermore, almost same results were obtained under the assumption (case 2) that the surface roughness effectively increased an average thickness d_{OH} of the Mg(OH)$_2$ layer without consideration of the morphology factors (or with s=1). Since both cases 1 and 2 may correspond to the extreme

cases of the film structure, the conclusions obtained here are reasonably considered to be applicable to the real film structure which may be in a situation between cases 1 and 2. It should be noted that the above density ratios of the

Table I. Surface morphology factor s and spectral intensity ratios of I_{HBE} to I_{LBE} of the O1s peak and the Mg2p to O1s peak, I^{Mg}/I^O, taken from single-crystalline MgO and the MgO films deposited under various conditions of the substrate temperature (RT or 723 K) and (with or without) $\sim 3\times10^{-5}$-Torr oxygen supply. Density ratios of Mg to O in the deposited MgO film (represented as MgO$_x$), D_{OX}^{Mg}/D_{OX}^{O}, under consideration of a morphology factor s (case 1) and the average thickness of the sputter-induced contaminant layer d_{OH} (case 2) are estimated for each sample.

Film deposition Conditions	RT, O$_2$	RT	723K, O$_2$	723K	Single MgO
I_{HBE}/I_{LBE}	0.50	0.23	0.24	0.35	0.20
I^{Mg}/I^O	0.080	0.085	0.071	0.068	0.082
fraction s (case 1)	0.84	0.98	0.97	0.91	1
D_{OX}^{Mg}/D_{OX}^{O} (case 1)	1.11	1.06	0.86	0.83	1
d_{OH} in nm (case 2)	0.34	0.17	0.18	0.25	0.15
D_{OX}^{Mg}/D_{OX}^{O} (case 2)	1.09	1.06	0.86	0.82	1
RMS in nm	66	2.5	-	25	-

RT : Room Temperature

underlying MgO$_x$ films deposited were not self-consistently estimated because the changes in the atomic composition of the films at least vary the concerned escape depths of photoelectrons. However, since the errors of the present analysis may be a few percents, and the structures considered differ from the real situations, more precise calculations may not be so meaningful. Furthermore, the composition changes estimated were less than 20 % in the worst case, suitable self-consistent corrections to the present values should not be very large. Thus, the estimated

density ratios are sufficiently meaningful.

4. Conclusion

We have investigated the morphology and composition of MgO thin films variously deposited on diamond (100) by means of electron beam evaporation method. The morphology observations by AFM indicated that the most flat and continuous film was grown at room temperature without oxygen supply, the roughness of which was even lower than the diamond substrate. The RT-deposited films in oxygen ambient were consisted of island shape domains, which remarkably increased the film roughness. The film growth rate and surface roughness increased with oxygen supply. It is found from the XPS spectral analysis that slightly O-rich films appeared in HT-deposited specimens while almost stoichiometric or slightly Mg-rich films were obtained for the RT-deposited films. Furthermore, the RT (without O_2)-deposited film had the closest composition the single-crystalline MgO. Consequently, it is concluded that the most flat and stoichiometric MgO film was grown at RT without O_2 supply on the CVD diamond (100) surface although the surface reactivity was higher, compared with the HT-deposited films. It is suggested that a peroxide layer was unintentionally formed in air on the surface of MgO films and single-crystalline MgO while in a ultra-high vacuum chamber, a hydroxide layer with a thickness of < 1.5 monolayer was formed on the ion etched surfaces. The thickness of these unintentionally formed layers was well correlated with the surface roughness and crystallinity of the MgO films deposited.

Reference

[1] M.C. Wu, J.S. Corneille, C.A. Estrada, J.W. He, D.W. Goodman, Chem. Phys. Lett. Vol. 182, p. 472, 1991.

[2] M. Baumer, D. Cappus, H. Kuhlenbeck, H.J. Freund, G. Wilhelmi, A. Brodde, H. Neddermeyer, Surf. Sci. Vol. 253, p. 116, 1991.

[3] D.K. Fork, K. Nashmoto, T.H. Geballe, Appl. Phys. Lett. Vol. 60, p. 1621, 1992.

[4] K. Nashimoto, D.K. Fork, T.H. Geballe, Appl. Phys. Lett. Vol. 60, p. 1199, 1992.

[5] L.S. Hung, C.W. Tang and M.G. Mason, Appl. Phys. Lett. Vol. 70, p. 152, 1997.

[6] L.H. Tjeng, A.R. Vos and G.A. Sawatzky: Surf. Sci. Vol. 235, p. 269, 1990.

[7] A.I. Boldyrev and J. Simons, J. Chem. Phys. Vol.100, p. 8023, 1996.

[8] D. Peterka, C. Tegenkamp, K.M. Schröder, W. Ernst, H. Pfnür, Surf. Sci. Vol. 431, p. 146, 1999.

[9] J.S. Corneille, J.W. He, D.W. Goodman, Surf. Sci. Vol. 306, p. 269, 1994.

[10] X.D. Peng and M.A. Barteau, Surf. Sci. Vol. 233, p. 283, 1990.

[11] S.M. Lee, H. Murakami and T. Ito, Appl. Surf. Sci. Vol. 175-176, p. 517, 2001.

[12] L.S. Hung, L.R. Zheng, T.N. Blanton, Appl. Phys. Lett. Vol. 60, p. 4129, 1992.

[13] J. Jupile, P. Dolle, M. Besancon, Surf. Sci. Vol. 260, p. 271, 1992.

[14] H.H. Huang, X. Jiang, H.L. Siew, W.S. Chin, W.S. Sim, Surf. Sci. Vol. 436, p. 167, 1999.

[15] Z.L. Wang, J. Bently, E.A. Kenik, L.L. Horton and R.A. Mckee, Surf. Sci. Vol. 273, p. 88, 1992.

[16] R. Martinez and M.A. Barteau, Langmuir Vol. 1, p. 684, 1985.

[17] D. Briggs and M.P Seah, Practical Surface Analysis, second edition, p. 247, 1990.

[18] D.R. Penn, J. Electron. Spectrosc. Relat. Phenom. Vol. 9, p. 29, 1976.

[19] D.J. Dwyer, S.D. Cameron, J.L. Gland, Surf. Sci. Vol. 159, p. 430, 1985.

[20] S.M. Lee, T. Ito and H. Murakami, J. Mater. Res. Vol. 17, p. 1914, 2002.